Journal of the American College of Cardiology
© 2012 by the American College of Cardiology Foundation
Published by Elsevier Inc.

Vol. 60, No. 16, 2012
ISSN 0735-1097/$36.00
http://dx.doi.org/10.1016/j.jacc.2012.05.048

Quantitative Assessment of Mitral Regurgitation

Validation of New Methods

Paaladinesh Thavendiranathan, MD, MSc,* Dermot Phelan, MB Bch, PhD,* James D. Thomas, MD,* Scott D. Flamm, MD, MBA,*† Thomas H. Marwick, MD, PhD, MPH*†

Cleveland, Ohio

Accurate assessment of mitral regurgitation (MR) severity is important for clinical decision making, prognostication, and decisions regarding timing of surgical intervention. The most common method for noninvasive assessment of MR has been with 2-dimensional transthoracic echocardiography, which is often used as a qualitative tool. Several newer noninvasive modalities including 3-dimensional echocardiography, cardiac magnetic resonance imaging, and cardiac computed tomography have also become available for this purpose; however, their role in routine clinical practice is not clearly defined. In this review, we provide an overview of these newer modalities for quantitative assessment of MR severity. (J Am Coll Cardiol 2012;60:1470–83) © 2012 by the American College of Cardiology Foundation

Mitral regurgitation (MR) remains one of the most common valvular heart diseases (1). Patients with moderate to severe MR have a high likelihood of developing symptoms of left ventricular (LV) dysfunction, and the 5-year cardiovascular disease–related mortality rate in selected, untreated asymptomatic patients is up to 14% (2,3). Substantial progress in the surgical treatment of MR has improved life expectancy (3,4), but prognosis and decisions regarding timing of surgery depend on the accurate quantification of MR severity (3,5). Advances in 3-dimensional echocardiography (3DE), cardiac magnetic resonance (CMR) imaging, and cardiac computed tomography (CCT) have provided new tools for MR quantification (Table 1).

This review of MR quantification methods using newer imaging modalities focuses on the diagnostic and prognostic value and reproducibility of each technique by a systematic review of the existing literature, and the benefits and limitations of the various techniques. When available, the performance characteristics of the 2-dimensional echocardiographic (2DE) techniques are also described. With respect to 3DE, our review focuses on studies that have used contemporary real-time imaging rather than reconstructive 3DE techniques.

Literature Review

A MEDLINE (1980 to January 2012) search was performed by 2 of the authors independently, using the search terms *mitral regurgitation, quantification, 3D-echocardiography, cardiac magnetic resonance imaging, cardiac computed tomography,* and their variations as key words on the OVID search engine. The search was limited to studies in humans and published in the English language. All citations were screened for inclusion by using a hierarchical approach of assessing the title, abstract, and manuscript. Studies that used reconstructive 3DE, did not provide separate data for patients with MR, enrolled only pediatric patients, did not have a reference standard, or were reviews were excluded. References of all selected articles and relevant reviews were screened to identify additional studies.

Vena Contracta Area

Validation of VCA measurements by 3DE. Grading of MR severity using vena contracta is based on estimating the effective regurgitant orifice area (EROA). With 2DE this is mainly limited to a vena contracta width (VCW) measurement from a transthoracic parasternal long-axis or a long-axis transesophageal echocardiographic (TEE) view (6). Alternatively a vena contracta area (VCA) can be calculated using a shape assumption (7,8) or by obtaining a short-axis en face view of the MR jet for planimetry (9). However, 3DE (transthoracic and transesophageal) affords the ability to measure the VCA using 3D-color Doppler acquisition of the MR jet followed by multiplanar reformatting to obtain an en face view of the VCA (Fig. 1). Studies comparing this technique to various reference standards (Table 2) have uniformly demonstrated it to be more accurate than 2D VCW measurement of MR severity. A cutoff of 0.41 cm^2 using 3D-VCA to differentiate moderate from severe MR showed an 82% sensitivity and 97% specificity (10). Because this technique is relatively new, its test–retest characteristics,

From the *Department of Cardiology, Heart and Vascular Institute; and the †Department of Radiology, Imaging Institute, Cleveland Clinic, Cleveland, Ohio. All authors have reported that they have no relationships relevant to the contents of this paper to disclose.

Manuscript received March 13, 2012; revised manuscript received May 7, 2012, accepted May 10, 2012.

prognostic value, threshold for severity classifications, and multicenter studies of accuracy and reproducibility remain undefined.

Benefits and limitations of 3D VCA measurements. Most studies assessing MR severity using 3DE are based on VCA measurements (Table 2). The most important benefit of this method is that the EROA is measured without any flow or geometric assumptions. This is especially important in functional MR (in which MR occurs along the length of the valve coaptation), and in other cases in which the regurgitant orifice is noncircular (7,8,11). 3D-VCA measurements appear accurate even in asymmetric regurgitant orifices, unaffected by the etiology or eccentricity of MR (8,10–14), although 2DE was used as reference standards in all but 4 studies (8,12,15,16). The 3D-VCA technique may reclassify patients into more accurate MR severity classes when compared to 2D-EROA or VCW (10,12,13).

The 3D-VCA technique has several limitations. The limited spatial resolution of the reconstructed image poses a particular problem with small regurgitant orifice area (10,14) but may not be as important in moderate to severe MR. A comparison of the apical to parasternal acquisition where the measurement of the VCA would be made in the axial plane has not shown significant difference in accuracy (14). Second, the choice of the systolic frame affects VCA measurement, depending on MR etiology (17,18), resulting in interobserver variability (Fig. 1, Panel A2). A third limitation is that 3D-VCA is easily affected by the multiplanar reformatting process used to obtain the cross-sectional plane for planimetry. This is particularly challenging when the regurgitant jet is highly eccentric, as cropping the regurgitant jet in a nonorthogonal manner can overestimate VCA. Although 1 study suggests that the VCA may be preserved over a distance of 5 to 10 mm distal to the orifice (19), in our experience, small variations in this location of the VCA measurement (Fig. 1, blue plane) can significantly change the area (Fig. 1, Panel B2). In addition, the measurement can be affected by color bleeding into the grayscale image, resulting in overestimation of VCA. Therefore, calibration of results from various cropping planes with other severity data is necessary in each laboratory before this technique can be clinically applicable. Fourth, while this method is less time-consuming than other techniques, the post-processing still requires a significant time commitment (up to 2 minutes in experienced hands) and expertise. Whether this will prove clinically practical in a busy echocardiography laboratory remains to be determined. Finally, the use of stitched 3D volumes predisposes to stitching artifact, which will affect the accuracy of the measurements. Although using nonstitched 3D acquisitions may help to overcome this problem, this technique is still often limited by temporal and spatial resolution.

Validation, benefits, and pitfalls of VCA measurements by CMR and CCT. With CMR cine-imaging, high-velocity flow across the regurgitant orifice causes a flow void due to dephasing of protons (Fig. 2) that can be potentially used for VCW (Figs. 2A and 2B) or VCA measurements. This flow void is typically better seen with fast gradient recalled echo (GRE) (Fig. 2B) cines with longer echo times (20) than the more commonly used steady-state free precession (Fig. 2A) cines that have lower sensitivity to flow due to short repetition time and echo times. Although not formally referred to as *VCA*, the regurgitant flow area at the mitral valve has been shown to be measurable with short-axis GRE cines using the flow void (21) or with through-plane phase contrast (PC) imaging (Figs. 2C to 2D) (22). In the first study, the measured area clearly differentiated MR severity categories when compared to echocardiography or ventriculography (21), whereas in the second study, good correlation (r = 0.82) was seen with EROA by echocardiography, with areas of 0.27 and 0.92 cm^2 differentiating mild from moderate and moderate from severe MR, respectively (22). Despite these data, the VCA technique is not commonly used clinically due to limitations such as through-plane motion of the slice position and partial volume effects making the measurement challenging. However, long-axis cines or short-axis PC imaging can be useful for the visual determination of the presence of MR and semiquantitative assessment of severity (20,23,24).

Valvular flow assessment is currently not possible with CCT imaging.

Abbreviations and Acronyms

2D = 2-dimensional
2DE = 2-dimensional echocardiography
3D = 3-dimensional
3DE = 3-dimensional echocardiography
AROA = anatomic regurgitant orifice area
CCT = cardiac computed tomography
CMR = cardiac magnetic resonance
EROA = effective regurgitant orifice area
GRE = gradient recalled echo
ICC = interclass correlation
Inter = interobserver variability
Intra = intraobserver variability
LV = left ventricular
LVOT = left ventricular outflow tract
MR = mitral regurgitation
PC = phase contrast
PFCR = proximal flow convergence region
PISA = proximal isovelocity surface area
RF = regurgitant fraction
RVol = regurgitant volume
SAX = short axis
SEE = standard error estimate
SSFP = steady state free precession
SV = stroke volume
TEE = transesophageal echocardiography
VCA = vena contract area
VCW = vena contract width

MR Volume and MR Fraction Measurements

Validation of MR volume and MR Fraction techniques by 3DE. Quantification of MR volume (RVol) and fraction (RF) using 3DE can be performed in several ways. The 3D-VCA (discussed earlier) or 3D proximal isovelocity surface area (PISA) based EROA or anatomic regurgitant orifice area (AROA; both discussed subsequently) coupled with the MR velocity time integral from continuous wave Doppler can be

Table 1 New Methods for Quantitative Assessment of MR: Clinical Use, Advantages, and Disadvantages

Modality	Clinical Use	Advantages	Disadvantages
3DE	Multiplanar reformatting of volumetric data to assess: VCA EROA using 3D PISA Anatomic regurgitation orifice area Color Doppler based RVol and RF quantification	Greater portability and availability Ability to reformat data as desired Multiple methods to assess MR severity	Lower CNR and SNR Stitching artifact Low temporal resolution with single heartbeat data Time-consuming reconstructions Acoustic window limitations
CMR	Indirect measurement of RVol and RF using: LV and RV stroke volumes Phase contrast imaging at the mitral valve and aorta Combination of above techniques Direct measurement of RVol with phase contrast imaging Direct planimetry of AROA	Excellent CNR and SNR Reproducible LV volume measurements Phase contrast imaging incorporates flow from entire orifice Multiple methods to confirm findings No acoustic window limitations	Not widely available Dedicated imaging planes required that can be time-consuming Significant experience necessary Contraindications in some patients Limited accuracy and reproducibility data
Cardiac CT	LV and RV stroke volumes to measure RVol Direct measurement of AROA	Highest spatial resolution, CNR, SNR No acoustic window limitation	Poor temporal resolution Cannot assess flow Radiation exposure

3D = 3-dimensional; 3DE = 3-dimensional echocardiography; AROA = anatomic regurgitation orifice area; CMR = cardiac magnetic resonance imaging; CNR = contrast-to-noise ratio; CT = computed tomography; EROA = effective regurgitant orifice area; LV = left ventricular; MR = mitral regurgitation; PISA = proximal isovelocity surface area; RF = regurgitant fraction; RV = right ventricular; RVol = regurgitant volume; SNR = signal-to-noise ratio; VCA = vena contracta area.

used to calculate RVol similar to 2DE techniques. This RVol coupled with 3D LV stroke volume (SV) obtained using endocardial tracking of a 3D LV volume can be used to calculate RF. Alternatively, the 3D LV SV can be coupled with LVOT SV by 2DE to calculate RVol and RF.

A more novel method is to use 3D color Doppler to measure mitral inflow and LV outflow tract (LVOT) SV and to use the difference to obtain RVol (25). RF can be calculated as (RVol/Mitral inflow SV) × 100. This technique uses the velocity assignment intrinsic to color Doppler combined with the mitral annular and LVOT area (based on the space occupied by the color Doppler) to calculate SV at each orifice (Fig. 3) (25). This can be more accurate and reproducible than 2D pulsed-wave Doppler-based methods (25,26). Table 3 summarizes real-time 3DE studies for SV quantification across the mitral valve and/or LVOT in adults; additional studies have confirmed the accuracy of this technique solely in pediatric patients

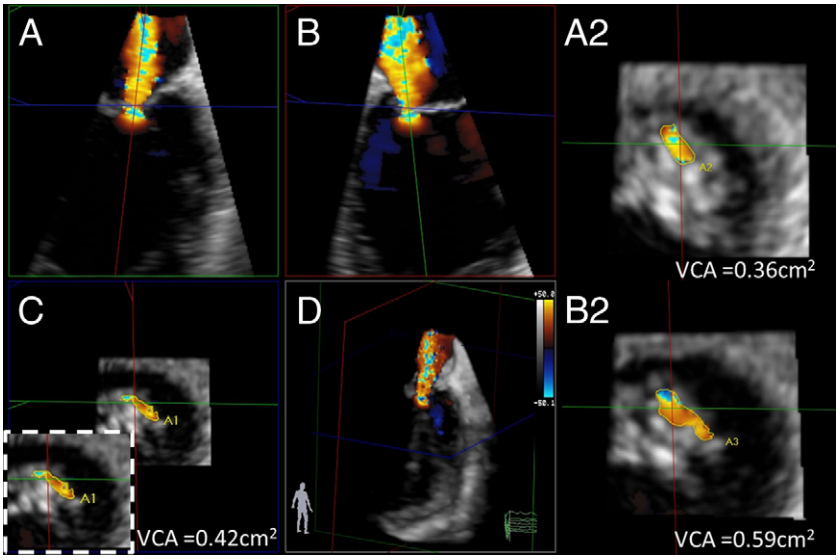

Figure 1 VCA Measurement Using 3D Color Full-Volume Acquisition by TEE

(A and B) Multiplanar reformatting to obtain the best view of the regurgitant jet and the vena contracta. **(C)** En face view of the vena contracta area (VCA) with planimetry **(A1)**. **(D)** Reformatted 3-dimensional (3D) volume illustrating the regurgitant jet. **A2 and B2** illustrate the effect of a change in systolic phase **(A2)** and the location of the *en face* **(blue)** plane, respectively, on the VCA measurement. TEE = transesophageal echocardiography.

Table 2 Real-Time 3DE Studies of the Accuracy and Reproducibility of the VCA Technique for MR Quantification and the Relevant 2D Methods Compared

First Author, Year, (Ref. #)	3DE Method	2D Method Compared	Reference Method	N	Agreement	Accuracy	Reproducibility	2D Method Results
Zeng et al., 2011 (10)	TTE, apical window	PISA EROA*; VCW	2DE-based mild/moderate/severe MR	83	r = 0.88 with MR severity grade; 0.88 with 2D EROA	AUC 0.96 (to differentiate moderate vs. severe MR)	Inter: 0.03 ± 0.11 cm^2†; intra: 0.04 ± 0.09 cm^2†	2D EROA r = 0.86, AUC 0.95, VCW r = 0.83, AUC 0.94 (to differentiate moderate vs. severe MR); 31.3% of patients upgraded to more severe MR with 3D VCA vs. 2D EROA
Marsan et al., 2011 (16)	TTE, apical window, 3D VCA based RVol	—	3D, 3-directional velocity encoded cine CMR RVol	52	r = 0.93	Bias −0.7 ± 6.5 ml/beat†	—	—
Shanks et al., 2010 (12)	TEE, 3D VCA based RVol	TEE 2D PISA EROA based RVol; VCW 2D from mid-esophageal 4CH view	CMR RVol	30	96.6% agreement with MR severity grade by CMR	RVol (ml/beat) 63.2 ± 41.3 (3D) vs. 65.1 ± 42.7 (CMR)	Mean inter difference: −0.013 ± 0.14 cm^2†; intra: 0.011 ± 0.16 cm^2†	2D RVol 53.2 ± 35.3 ml/beat; MR severity misclassified in 33% of patients compared to CMR using RVol or VCW; 2D EROA underestimated by 26% compared to 3D VCA
Marsan et al., 2009 (8)	TTE, apical window, 3D VCA based RVol	2D RVol by EROA using VCW measurements and shape assumption	3D, 3-directional velocity encoded cine CMR for direct measure of RVol	64	RVol r = 0.94	–0.08 ± 7.7 ml/beat† (p = NS)	—	RVol circular EROA −2.9 ± 15.1 ml/beat†; elliptical EROA −1.6 ± 10.3 ml/beat† (p < 0.05 for both)
Yosefy et al., 2009 (13)	TTE, parasternal window	VCW from PLAX view	EROA by 2D volumetric method	45	r^2 = 0.86, SEE 0.02 cm^2	VCA vs EROA bias 0.04 ± 0.06 cm^2‡ (p = NS)	Inter: r = 0.95, SD of differences 0.03 cm^2; intra: r = 0.97, SD of differences 0.01 cm^2	r^2 vs. 2D EROA = 0.81; MR severity misclassified in 45% of patients with eccentric MR; VCW inter = 0.95 (SD 0.06 cm)
Little et al., 2008 (14)	TTE, parasternal and apical windows§	2D VCW PLAX	EROA by 2D volumetric method* and MR grade as per ASE	61	r = 0.85 with EROA (all patients), MR grades 1–2 r = 0.2, MR grades 3–4 r = 0.80	3D VCA 0.29 ± 0.18 cm^2 vs. 2D EROA 0.29 ± 0.24 cm^2; among MR severity categories there was overlap in 3 VCA	Inter: r = 0.96, mean bias 0.05 ± 0.02 cm^2; no intra	2D VCW vs. EROA r = 0.67 (all patients), for MR grades 1–2 r = 0.68, for grades 3–4 r = 0.18
Kahlert et al., 2008 (7)	TTE, apical window	VCW in apical 4CH, 2CH, and mean. VCA from each view assuming a circle, Biplane elliptical VCA	2D PISA EROA with hemispheric (EROA HS) or hemielliptic (EROA HE) approach (using MPR of 3D color Doppler)	57	r = 0.96 (vs. EROA HE); r = 0.93 (vs. EROA HS)	3D VCA larger vs. EROA HE = 0.09 ± 0.14 cm^2‡; vs. EROA HS = 0.20 ± 0.20 cm^2‡	Inter r = 0.97, bias 0.04 ± 0.09 cm^2‡; no Intra	Compared to PISA EROA VCW r ranged from 0.63–0.85 (best was mean VCW), and VCA r = 0.59–0.90; best VCA estimate by Biplane vs. EROA HE +0.09 ± 0.20 cm^2‡; inter VCW 4CH r = 0.97, bias 0.02 ± 0.05 cm,‡ VCW 2CH r = 0.94, bias 0.02 ± 0.04 cm‡
Iwakura et al., 2006 (11)	TTE, apical window	2D PISA* EROA	Volumetric EROA using LVOT Doppler, Biplane Simpson's, and MR VTI, and 2D PISA EROA*	106	r = 0.91 vs. volumetric EROA and r = 0.93 vs. PISA EROA	Mean 3D VCA 0.28 ± 0.27 cm^2, volumetric EROA 0.22 ± 0.22 cm^2, PISA EROA 0.20 ± 0.18 cm^2	Intra: 8.6 ± 6.6%†; inter: 9.0 ± 6.1%†	Comparison to volumetric 2D PISA EROA r = 0.89; PISA EROA smaller than volumetric method and 3D VCA
Khanna et al., 2004 (15)	TTE, apical and parasternal windows‖	VCW, VCA (circular assumption)	Cardiac catheterization grading 1–3	44	Spearman r = 0.88	—	Inter r^2 = 0.99; intra r^2 = 0.97	VCW Spearman r = 0.51; VCA Spearman r = 0.55

*Based on hemispheric assumption. †Difference reported as mean ± 2 SD. ‡Difference reported as mean ± 1 SD. §Comparison data were presented for the apical window only. ‖The better of the apical or parasternal window was used to measure the VCA.

2CH = 2 chamber; 2DE = 2-dimensional echocardiography; 4CH = 4 chamber; ASE = American Society of Echocardiography; AUC = area under the curve; **HE = hemielliptic; HS = hemispheric**; ICC = interclass correlation; inter = interobserver variability; intra = intraobserver variability; ns = not significant; PLAX = parasternal long axis; SD = standard deviation; SEE = standard error of the estimate; TEE = transesophageal echocardiography; VCW = vena contract width; volumetric EROA = (mitral inflow stroke volume [SV] by area and pulsed-wave [PW] Doppler OR Biplane Simpson's – left ventricular outflow tract [LVOT] flow by area and PW Doppler)/MR velocity time integral [VTI]; other abbreviations as in Table 1.

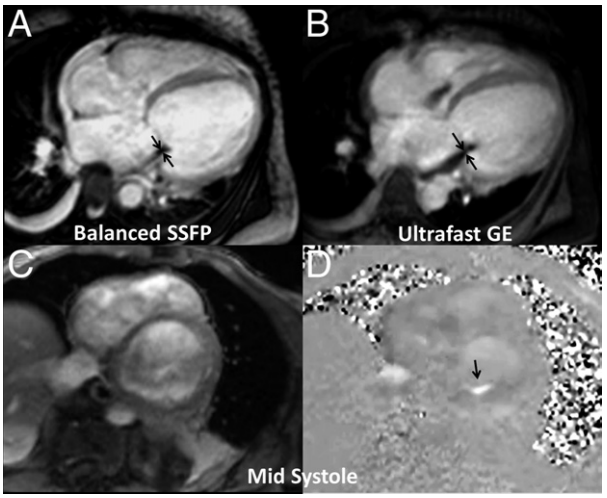

Figure 2 **VCW and VCA Measurements by CMR**

Cardiac magnetic resonance imaging (CMR) vena contracta width (VCW) measured on **(A)** a balanced steady-state free precession (SSFP) and **(B)** ultrafast gradient echo (GRE) imaging. The vena contracta is best seen in the ultrafast GRE image. Magnitude **(C)** and phase **(D)** imaging with an *en face* view of the vena contracta **(arrow)** from which the VCA can be measured. Abbreviation as in Figure 1.

(27,28). To date, however, most studies (25–27,29–31) have examined SV only at the mitral annulus or LVOT separately, with only 1 study having assessed simultaneous measurement of mitral and LVOT SV from a single 3D volume (25).

Benefits and limitations of RVol and RF quantification techniques by 3DE. There are several merits to the novel 3D color Doppler technique for the quantification of SV. In contrast to pulsed-wave Doppler sampling of velocities over a sample volume of 2 to 5 mm in diameter, this method integrates flow velocities across the entire mitral or aortic orifice to calculate SV (25,26). Furthermore, no assumptions are made about the LVOT or mitral annular geometry. An automated angle correction technique or a hemispheric sampling plane is used to overcome the angle dependence of color Doppler flow and a manual or automated de-aliasing algorithm to overcome color Doppler aliasing.

Although ideally suited to measure MR RVol and RF (Figs. 3D to 3F), there is only preliminary work in this area (32). The major limitation is that it is only valid in the absence of other concomitant valvular disease or intracardiac shunting. The accuracy of the described de-aliasing algorithms is yet to be tested in the context of increased velocities across the mitral or aortic valves. With the exception of 1 study in which SV for the mitral and aortic valve for multiple heartbeats was obtained in <60 s (25), a significant time commitment is required to quantify SV for each valve for a single cardiac cycle. Also the frame rate of 3D color Doppler acquisitions is still limited and data

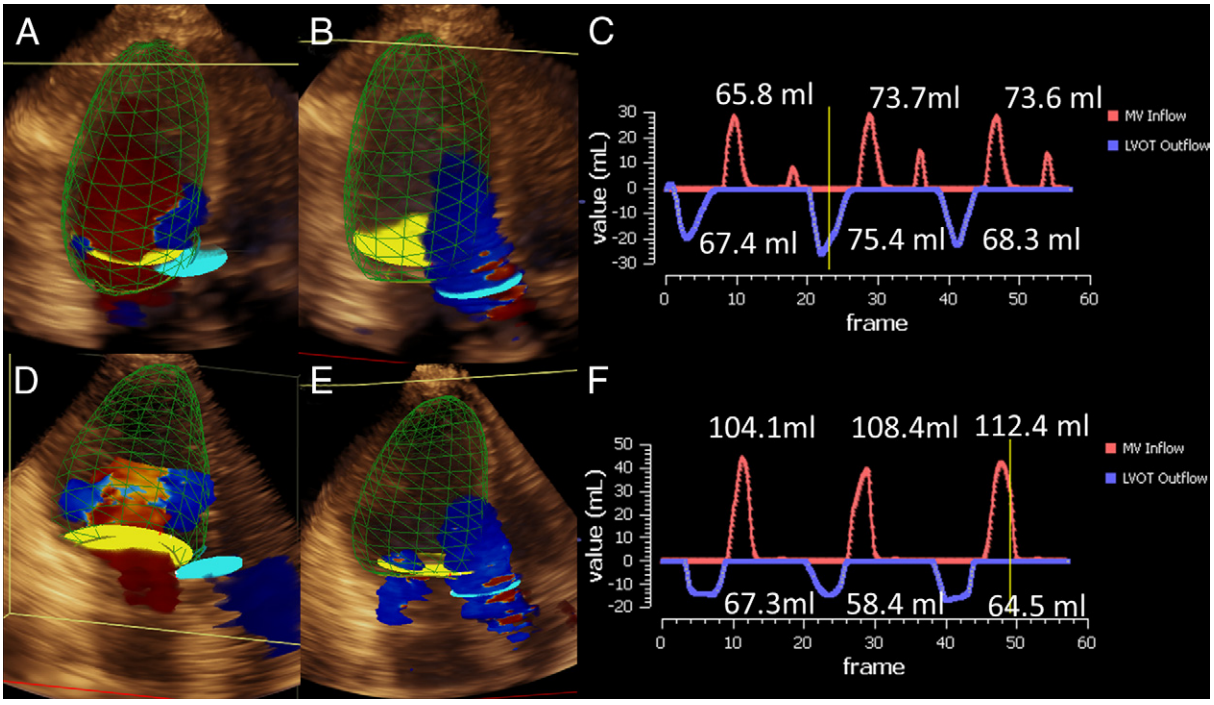

Figure 3 **3D Color Doppler Based Stroke Volume Quantification**

(A to C) A patient without mitral regurgitation (MR) in whom the mean mitral inflow and aortic outflow stroke volumes were similar.
(D to F) A patient with MR in whom the mean mitral regurgitant volume was 45 ml (mean mitral inflow, 108 ml; mean aortic outflow, 63 ml).

Table 3 Real-Time 3DE Studies of the Accuracy and Reproducibility of the Mitral and LVOT SV Quantification and the Relevant 2D Methods Compared

First Author, Year (Ref. #)	3DE Method	2D Method Compared	Reference Method	N	Agreement	Accuracy	Reproducibility	2D Method Results
Thavendiranathan et al., 2012 (25)	SV across mitral and aortic valve in a single 3D volume, TTE	2DE PW based SV across mitral and aortic valve	CMR	44	Mitral inflow r = 0.91; LVOT r = 0.93	Bias mitral SV = 1.1 ± 18.9 ml*‡; LVOT SV = 0.7 ± 17.8 ml‡	MV and LVOT inter 4.1 and 4.5%†; intra 2.4 and 2.0%†	SV MV r = 0.66, LVOT r = 0.62, bias SV MV 10.6 ± 36.0 ml‡; LVOT 10.6 ± 40.3 ml‡; inter MV inflow 14.1%†; LVOT 9.6%†
Pemberton et al., 2008 (30)	SV across LVOT, TTE	—	CMR	12 (65 measures)	r^2 = 0.83	Underestimation of SV by 5.7 ± 8.8 ml*	Inter r^2 = 0.97, bias 0.27 ± 7.9 ml*	—
Lodato et al., 2007 (26)	SV across mitral and aortic valves using separate 3D volumes, TTE	2DE PW based SV across LVOT and mitral valve	Cardiac catheterization	47	Aortic valve r = 0.94, mitral valve r = 0.93	Aortic valve SV −1.8 ± 16.8 ml‡; mitral valve SV −0.2 ± 15.6 ml‡	Aortic valve inter 13.7%†; intra 5.2%†	Aortic valve r = 0.78, mitral valve r = 0.75, aortic valve SV −8.6 ± 36.2 ml‡; mitral valve SV +10.0 ± 26 ml.‡ aortic valve inter 11.5%,† intra 5.3%†
Pemberton et al., 2005 (31)§	SV across LVOT only, TTE	—	2DE pulsed Doppler based SV	50	r^2 = 0.90; SEE 6.98 ml	LVOT SV −1.8 ± 7.9 ml*	Inter r^2 = 0.91, mean difference −1.6 ± 5.8 ml*	—

*Difference reported as mean ± 1 SD. †Expressed as summed quotient of the difference and the means of individual values. ‡Difference reported as mean ± 2 SD. §Had adult and pediatric patients (23 adult, 27 pediatric).
MV = mitral valve; other abbreviations as in Tables 1 and 2.

accuracy is potentially reduced at higher heart rates. Finally, the accuracy of this technique can be affected by lateral resolution, tissue priority settings, and incomplete color Doppler acquisitions at the mitral valve or LVOT. Therefore, further studies are necessary before this technique can be used clinically for MR quantification.

Validation of RVol and RF quantification techniques by CMR. Mitral RVol and RF measurements using CMR can be obtained using direct or indirect methods. The direct method utilizes PC imaging to measure RVol using SAX through-plane images at the mitral valve (Fig. 4A) (33). The RF is then calculated as RVol divided by the LV-SV calculated from planimetry of SAX slices. The indirect methods use: 1) the difference in LV-SV by planimetry of SAX cines and aortic SV by PC imaging (Fig. 5B) (34–36); 2) the difference in LV- and RV-SV by planimetry of SAX cines of the LV and RV (33,37–39); 3) the difference in mitral inflow SV across the mitral valve (Fig. 4B) and aortic forward SV with PC imaging (Fig. 4C) (40); or 4) other less commonly utilized combinations of PC and volumetric analyses.

The use of the difference in SVs by LV short-axis planimetry and aortic PC imaging is more practical and reproducible than the other methods (38). Furthermore, aortic PC technique can potentially account for any aortic regurgitation present. Currently the only work that provides RF categories to grade MR severity using CMR is based on this technique (41). However, these categories were obtained using nonquantitative echocardiographic parameters (41) as the reference standard and require further validation. To date, no studies have addressed the prognostic significance of MR quantification using CMR, test–retest variability, or its accuracy and reproducibility in a multicenter study.

Benefits and limitations of RVol and RF quantification techniques by CMR. CMR is considered the reference standard for the assessment of ventricular volumes and EF, as the endocardial contours can be drawn with confidence and the volumes and EF calculated without geometric assumptions. Employing PC imaging, aortic SVs are calculated using velocities from the entire orifice (without needing to assume constant transorifice flow profile as in echocardiography with pulsed-wave Doppler). Furthermore, the RVol and RF are calculated without any hemodynamic or shape assumptions and are not affected by the direction of the MR jet (except for the direct method) or the orifice geometry. Finally, the comparable spatial resolution, but superior signal- and contrast-noise resolution, of CMR make these measurements reproducible and amenable to serial assessments.

Despite the enthusiasm for using CMR for MR quantification, there are limited data on accuracy; several of the CMR studies shown in Table 4 were not specifically performed for the validation of that technique, nor did they have an independent reference standard (33,34,36,38). Furthermore, the described techniques have some limitations. First, the indirect quantification methods can be challenging and less accurate if multiple valvular lesions or intracardiac

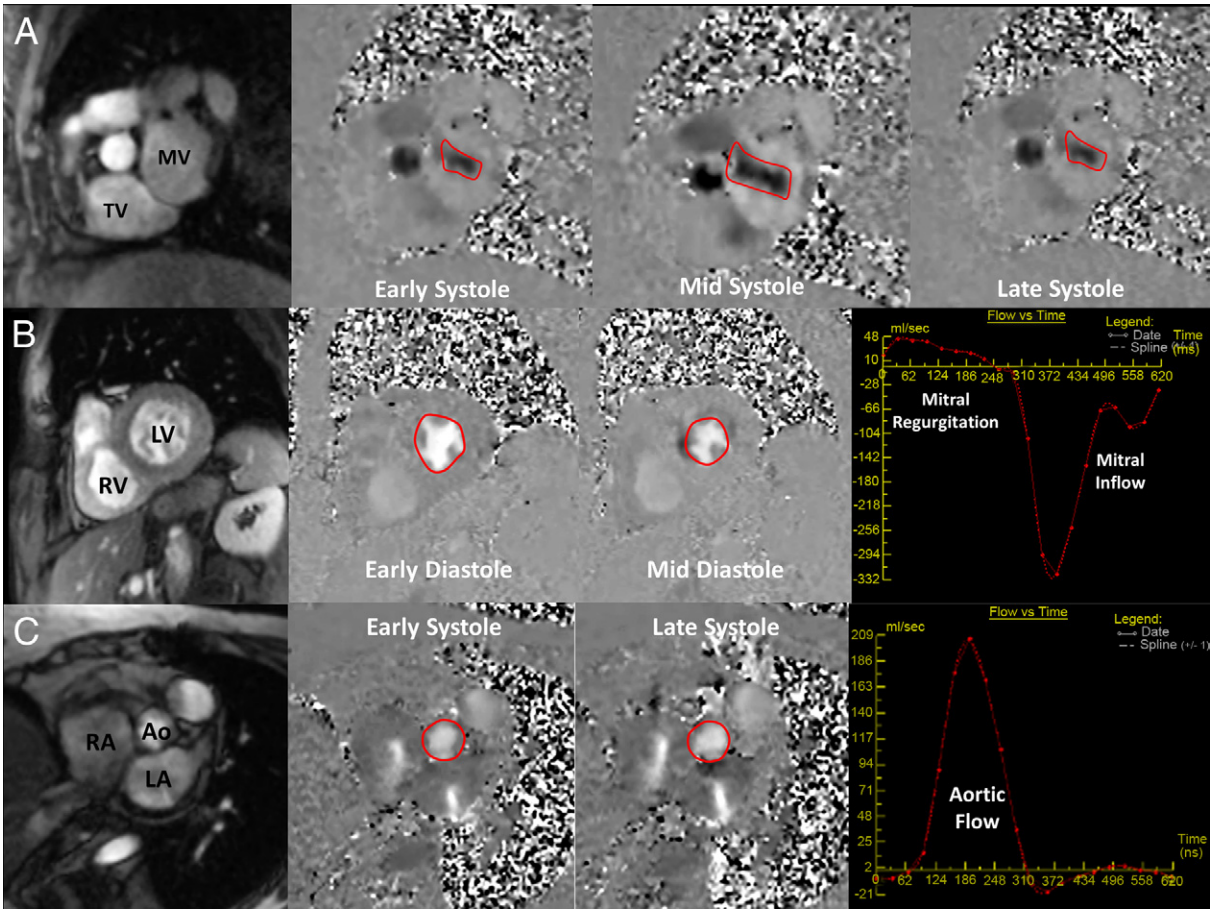

Figure 4 **CMR Phase Contrast Acquisitions**

(A) Phase contrast through plane imaging at the mitral valve, with a magnitude **(left)** and 3 phase images with contours of the mitral regurgitant jet **(black)** to directly quantify the regurgitant volume (MR curve, **panel B, right)**. **(B)** Mitral inflow magnitude and 2 phase images with planimetry of the mitral valve **(red)**, and mitral inflow and mitral regurgitation flow curves. **(C)** Aortic magnitude and 2 phase images with planimetry of the aorta and aortic flow curve. Ao = aorta; LV/RV = left ventricle/right ventricle; RA/LA = right atrium/left atrium; TV/MV = tricuspid/mitral valve.

shunting is present. Second, the manual planimetry of both the LV and RV, or the mitral valve in each systolic or diastolic frame (Figs. 4A and 4B), can introduce inter- and intraobserver variability. Direct measurement of RVol from PC imaging (Fig. 4A) is attractive as it minimizes the cumulative error that can occur from using 2 separate measurements. However, further validation of this technique is necessary before clinical use. Third, MR-RVol may be overestimated if there is inconsistency in LV endocardial contouring; namely, if the trabecular and papillary muscles are treated asymmetrically such that they are included in the blood volume at end-diastole, but excluded at end-systole, resulting in overestimation of the LV SV. Fourth, PC sequences are subject to phase offset errors due to inhomogeneity in the magnetic field (42) and can cause errors in SV computations. Various methods to overcome these errors have been suggested but can be impractical or inaccurate (43). Fifth, the PC sequence most commonly used is a 1-dimensional, 1-directional technique and hence SVs can be underestimated if the flow is not at least nearly orthogonal to the slice position. In addition, these sequences do not account for through-plane motion of the valve plane, which can lead to underestimation of RVol. These concerns have resulted in an interest in the use of 3D, 3-directional PC imaging sequences (8) and retrospective valve tracking, although experience with these techniques is limited and imaging is time intensive. Finally, it is also unclear if the RVol and RF cut-offs suggested in the echocardiographic guidelines can be applied to the CMR measurements to classify MR severity, and our experience suggests that lower value cutoffs for CMR may be more appropriate. Further studies are therefore needed.

Validation, benefits, and limitations of RVol and RF quantification by CCT. Current CCT technology does not allow flow measurements across the valves. However, RVol and RF can be measured using LV and RV contouring (37) similar to CMR. The only published study (37) showed good agreement in RVol and RF with CMR and

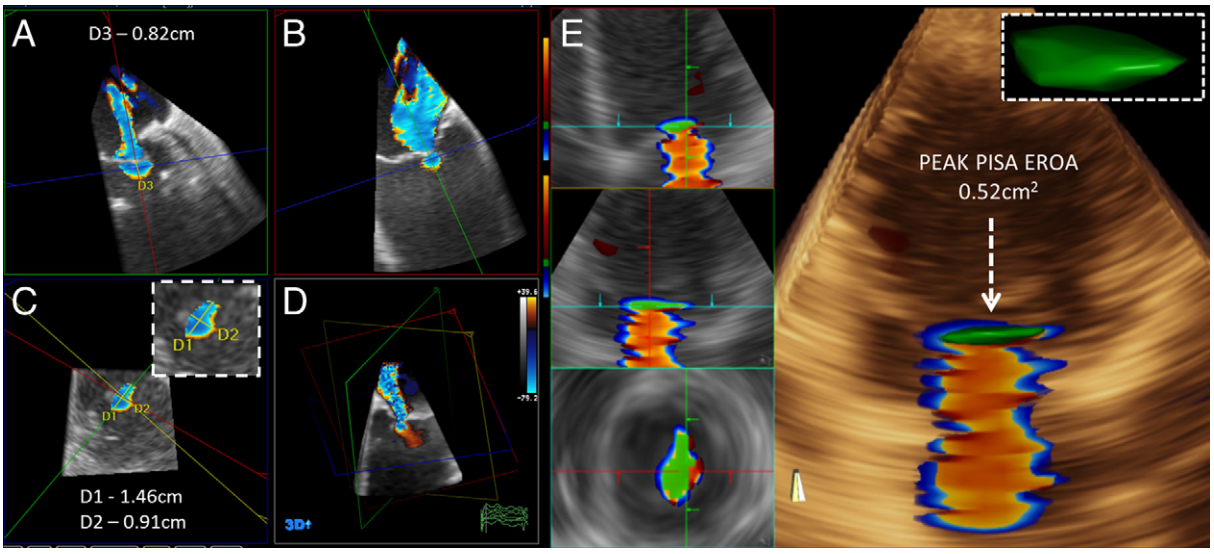

Figure 5 **3D PISA Quantification**

Proximal isovelocity surface area (PISA) quantification using **(A to D)** linear 2-dimensional (2D) measurements and **(E)** automated 3D surface detection. **(A)** Radius, **(C)** length **(D1)**, and width **(D2)** measured from 3D TEE using multiplanar reformatting of full-volume color Doppler acquisition **(D)** after decreasing the aliasing velocity. Automated 3D PISA detection and quantification using 3D transthoracic echocardiography **(E; green model** represents the 3D PISA).

echocardiography (Table 5). This technique requires a retrospectively gated acquisition with modification to contrast administration to ensure simultaneous opacification of the LV and RV. Using post-processing, software LV and RV volumes can be semiautomatically calculated or short-axis views can be generated identical to CMR for manual planimetry. Despite the feasibility of this technique, and excellent spatial resolution, CCT is still limited by a maximum temporal resolution of 75 ms (at best), and the need for retrospectively gated acquisition resulting in higher radiation exposure. Also, this technique will be inaccurate in the presence of multivalvular disease, hence necessitating an alternate modality to first rule out concomitant valvular lesions. Therefore, CCT would be the last resort for MR severity quantification in patients with poor echocardiography windows and/or a contraindication for CMR.

PISA (EROA, RVol, RF) and Anatomic Regurgitant Orifice Area

Validation of 3DE PISA and anatomic regurgitant orifice area. The anatomic severity of MR can be assessed by 3D color Doppler using the PISA technique or by direct planimetry of the AROA. The theoretical benefit of the 3D PISA technique is the ability to measure the 3D surface of the proximal flow convergence region (PFCR) without shape assumptions (44) or to obtain the largest radius of the PFCR using 3D navigation, possibly increasing the accuracy of the EROA calculation (Fig. 5) (44,45). Furthermore, 3DE (Table 6) has provided a better appreciation of the variability in the PFCR seen with different pathologies and geometric orifices and has illustrated the complexity of the PISA technique for MR quantification. Many of the studies in Table 6 have used 2DE techniques as the reference standard and hence are subject to the intrinsic limitation of these methods.

The direct planimetry technique requires reconstruction of the 3DE (B-mode) to obtain an en face view of the AROA. This method was first described with reconstructed 3D TEE (46,47) and more recently with real time 3D TEE (Table 6, Fig. 6). No studies to date have assessed the use of 3D TTE to measure the AROA. It is also important to remember that the AROA is theoretically larger than the EROA (19,48).

Benefits and limitations of PISA and AROA techniques by 3DE. Although 3D data can be used to measure the "true" radius (D3), length (D1), and width (D2) of the PFCR (Fig. 5) and to apply hemispheric or other-shaped assumptions, and although the use of 3D data may improve the accuracy of the EROA calculation, it still requires assumptions about the shape of the PFCR (44,49,50). Two studies have attempted to obtain a 3D surface area, one using measurement of multiple radial planes of the PFCR in an in vitro model to subsequently reconstruct the total surface area (51), and the second using multiple linear measurements to reconstruct the 3D surface area (52). Both methods are laborious and not practical in a busy clinical setting. There has been some recent work on automated 3D quantification of the PFCR (Fig. 5E) (32,53); however, further clinical validation is pending. Nonetheless, even with the 3D-surface area the issue of Doppler angle dependency (54) and the challenges of accounting for dynamic variations in EROA for RVol calculations will still exist

Table 4 CMR Studies Using Direct and Indirect Methods of Quantifying MR

First Author, Year (Ref. #)	Reference Method	N	Agreement	Accuracy	Reproducibility
Direct method using PC imaging					
Myerson et al., 2010 (33)	CMR RVol as difference of LV volumes by planimetry and aortic PC imaging	55	RVol r = 0.87	RVol bias 8.5 ± 44.1 ml*†; RF bias −5.5 ± 29.8%*†	—
Indirect method—planimetry of LV and PC imaging of aorta					
Buchner et al., 2008 (34)	RVol and RF by catheterization, (LV planimetry + thermodilution)	28	RF r = 0.89; RVol r = 0.84	—	—
Kizilbash et al., 1998 (36)‡	RVol and RF by TTE mitral and LVOT stroke volumes by PW Doppler	22 (18 with MR)	RVol r = 0.92; RF r = 0.82	RVol −3 ± 13ml§; RF −7 ± 11%§	—
Hundley et al., 1995 (35)	Catheterization (thermodilution and Fick + LV volume by area length method)	23 (17 with MR)	RVol index r = 0.97; RF r = 0.96	RVol index bias ~−0.1 ± 0.7* l/min/m^2, RF ~2 ± 12%*	Inter RF 10 ± 9%*
Indirect method—planimetry of LV and RV					
Myerson et al., 2010 (33)	CMR RVol as difference of LV volumes by planimetry and aortic PC imaging	55	—	RVol Bias −3.1 ± 30.8ml*‖; RF Bias −1.9 ± 20.6%*‖	—
Guo et al., 2009 (37)	MR severity categories by TTE color Doppler area (not per ASE guidelines)	49	CMR RF vs TTE MR grade Spearman r = 0.94, no RVol data	Agreement kappa for MR severity categorization by CMR vs echo = 0.91	Inter RVol¶ 6.7 ± 3.3%, RF 8.1 ± 4.4%§; intra RVol¶ 7.3 ± 4.7%, RF 9.1 ± 4.2%§
Kon et al., 2004 (38)	RF obtained from LV stroke volumes by planimetry and PC imaging of aortic flow	28	—	RF bias −1.6 ± 10.1%§, no RVol data	Intra RF −2.0 ± 6.7%§ inter 0.4 ± 8.8%§ Reproducibility of reference method: Intra RF 0.6 ± 4.8%§, inter 2.0 ± 7.7%§
Glogar et al., 1989 (39)#	RF from cardiac catheterization (LV planimetry + thermodilution)	20	RF MRI vs catheterization, r = 0.67 (all patients); r = 0.84 (13 patients with the best MRI images)	κ = 0.62 (agreement with catheterization for categorization into 3 RF classes, >50%, 20%–50%, and 0%–20%)	LV SV inter mean 7.0 ml (range 2–15 ml) RV SV inter mean 7.3 ml (range 6–8 ml)
Indirect method—PC imaging of mitral inflow and aortic outflow					
Fujita et al., 1994 (40)	TTE MR severity grade based on: color jet area, CW Doppler density, "increased" E velocity	19	r = 0.87 for RF, and 0.74 for RVol with echo severity grade	—	Inter RVol r = 0.99, SEE = 238ml/min, RF r = 0.98, SEE 4.1%

*Difference reported as mean ± 2 SD. †Comparison with RVol and RF with LV and RV planimetry method also available but not shown here. ‡The primary intention of this study was to assess the accuracy of the Doppler technique using MRI. §Difference reported as mean ± 1 SD. ‖Data also available for comparison with direct RVol method but not shown here. ¶Calculated as average of the difference between measures divided by the mean. #A 0.5-T magnet was used, and LV and RV were contoured using 4CH stacks.
CCT = cardiac CT; CW = continuous wave; HR = heart rate; κ= kappa; other abbreviations as in Tables 1 to 3.

(17,18,55). Also to date there is limited experience with this technique using TEE. Finally, 3D color Doppler imaging remains limited by acquisition volume rate, which can affect identification of the largest PFCR during systole.

The use of 3DE in planimetry of the AROA is attractive as unlike 2DE the 3D dataset can be reconstructed to obtain an en face view of the regurgitant orifice (Fig. 6). Planimetry can be used for multiple regurgitant orifices and added together, with no hemodynamic or shape assumptions necessary. However, given the contrast and spatial resolution limitations of 3DE, measurement of the AROA—especially of smaller orifices—is challenging (56). This is

Table 5 Cardiac CT Study for MR Quantification by LV and RV Planimetry

Study	Reference Method	N	Agreement	Accuracy	Reproducibility
Guo et al., 2009 (37)	1. CMR RVol and RF and 2. TTE based MR severity categorization*	49	Vs. CMR RVol r = 0.89, RF r = 0.91; vs. TTE MR severity grading r = 0.95	Agreement kappa with TTE MR severity categorization = 0.90; bias vs CMR RVol −1.0 ± 24.3ml; CMR RF 0.2 ± 15.4%†	Inter: RVol 4.8 ± 2.1%, RF 6.5 ± 3.4%‡; intra: RVol 6.9 ± 4.1%, RF 7.8 ± 3.6%‡

*Echocardiography severity grading cutoffs used were not as per ASE guidelines. †Mean ± 2 SD. ‡Mean ± 1 SD.
Abbreviations as in Tables 1 to 4.

Table 6 3DE Studies for 3D PISA and Anatomic Regurgitant Orifice Area (Last Row Only) Techniques

First Author, Year (Ref. #)	3D Method	2D Method Tested	Reference Method	N	Agreement	Accuracy	Reproducibility	2D Method Results
Matsumura et al., 2008 (50)	EROA using maximum radius of the 3D PISA TTE	—	EROA by 2D quantitative Doppler	54	Functional MR $r = 0.67$, MVP $r = 0.88$	In functional MR bias 0.18 ± 0.08 cm^2*; MVP -0.03 ± 0.09 cm^2*	3D PISA radius inter $r = 0.83$, intra $r = 0.89$, mean bias for PISA radius inter 0.05 cm; intra 0.06 cm	—
Matsumura et al., 2008 (52)	3D PISA EROA and RVol using hemispheric or hemiellipsoid assumption, TTE	—	EROA by 2D quantitative Doppler	30	Hemispheric PISA EROA $r = 0.69$, hemiellipsoid PISA EROA $r = 0.75$, no RVol data	Mean EROA and RVol underestimation for hemispheric PISA 0.18 cm^2 and 26.4 ml, hemiellipsoid 0.10 cm^2 and 14.5 ml (all, $p < 0.001$)	EROA hemisphere inter and intra $r = 0.90$ and 0.94, mean bias 0.07 and 0.03 cm^2, hemiellipsoid $r = 0.90$ and 0.97, bias 0.06 and 0.04 cm^2	—
Plicht et al., 2008 (45)	3D PISA based RVol using hemispheric or hemiellipsoid assumption, TTE and TEE	—	CMR RVOL	23	Hemispheric PISA RVol $r = 0.81$, hemiellipsoid PISA RVol $r = 0.89$	Bias vs MRI – Hemispheric PISA RVol -17.4 ± 9.4ml ($p < 0.05$), Hemiellipsoid PISA -11.7 ± 7.4 ml ($p < 0.05$)*	—	—
Yosefy et al., 2007 (44)	3D PISA EROA using linear measures and hemiellipsoid shape assumption, TTE	2DE PISA based EROA	EROA by 2D quantitative Doppler	40	3D vs. 2D EROA $r^2 = 0.87$	EROA 0.52 ± 0.17 cm^2 (3D) vs. 0.48 ± 0.25 cm^2 (reference) (p = ns). 3D EROA had 97% agreement with reference in classifying moderate to severe MR	EROA inter –5.3%†	2D EROA 0.34 ± 0.24 cm^2 ($p < 0.001$), $r^2 = 0.59$, 45% of patients with ≥ moderate to severe MR underestimated by 2D (inter 4.1%†; reference standard inter 7.3%†
Sitges et al., 2003 (49)	3D PISA EROA and RVOL using largest radius and hemispheric assumption, TTE	—	RVol volume as a difference of 3D LV SV and LVOT SV	22	RVol $r = 0.93$; EROA $r = 0.90$	RVol bias -4.8 ± 7.6 ml‡ ($p < 0.01$) and ROA bias 3.2 ± 5.2 mm^2‡ ($p < 0.01$)	Inter for largest radius $r = 0.90$, mean difference 0.4 ± 7.2%. Intra $r = 0.96$, mean difference 0.3 ± 5.6%.	—
Altiok et al., 2011 (56)	Direct planimetry of AROA using 3D zoom, TEE	—	2D PISA§, and 2D VCA‖	72	With PISA $r = 0.96$, SEE 0.058 cm^2; with VCA $r = 0.89$, SEE 0.105 cm^2	With PISA 0.01 ± 0.12‡, with VCA 0.03 ± 0.24‡	Inter 0.02 ± 0.12‡, $r = 0.96$; intra 0.01 ± 0.10‡, $r = 0.95$	—

*Mean ± 1 SD. †Variability was defined as the SD of the difference between the observers and expressed as percentage of the means. ‡Mean ± 2 SD. §Using hemispheric assumption; ‖VCA calculated using 2 πr^2 with average of 2 orthogonal vena contracta measurements. ROA = regurgitant orifice area; TTE = transthoracic echocardiography; other abbreviations as in Tables 1 to 5.

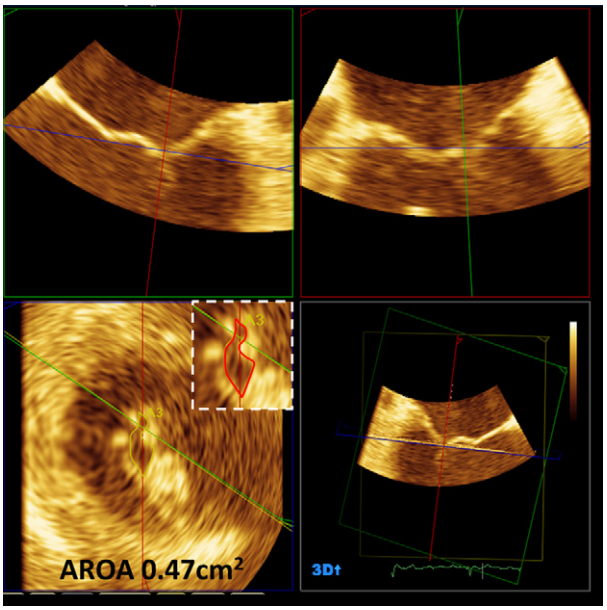

Figure 6 **Anatomic Regurgitant Orifice Area by 3DE**

Direct planimetry of anatomic regurgitant orifice area **(A3, bottom left panel)** using multiplanar reformatting of a 3D zoom acquisition using TEE. 3DE = 3D echocardiography; AROA = anatomic regurgitant orifice area.

further confounded by the fact that the measurement is made in the plane with the lowest spatial resolution (lateral resolution) unless a transgastric view in TEE or a parasternal long or short axis view with TTE is used (56). Also limitations described for the VCA measurement, such as choice of systolic frame, obtaining the best en face plane, and stitching artifacts, also apply (17,18). Finally, although a 3D volume is used to identify the AROA, the measurement is still made using a 2D plane. A recent study illustrated that the measurement of the AROA in 3D space using 3D modeling of the mitral valve may be a better alternative to quantify MR severity (48).

Validation of AROA by CMR and CCT. Although PISA is not feasible with CMR or CCT, the AROA can be measured directly by both (Fig. 7) although not commonly used clinically. Utilizing CMR, 3 studies have assessed the use of short-axis steady-state free precession and/or fast GRE cine images for planimetry of the AROA (Figs. 7A to 7C, Table 7) (22,34,57); 1 of these studies reported the reproducibility of this technique (34). Three small CCT studies, using 16 to 64 slice scanners, have examined direct planimetry of the AROA using an en face view of the regurgitant orifice from reconstructed 3D datasets (58–60) (Figs. 7D to 7F). The latter 3 studies showed moderate to good agreement with various reference standards (Table 7); however,

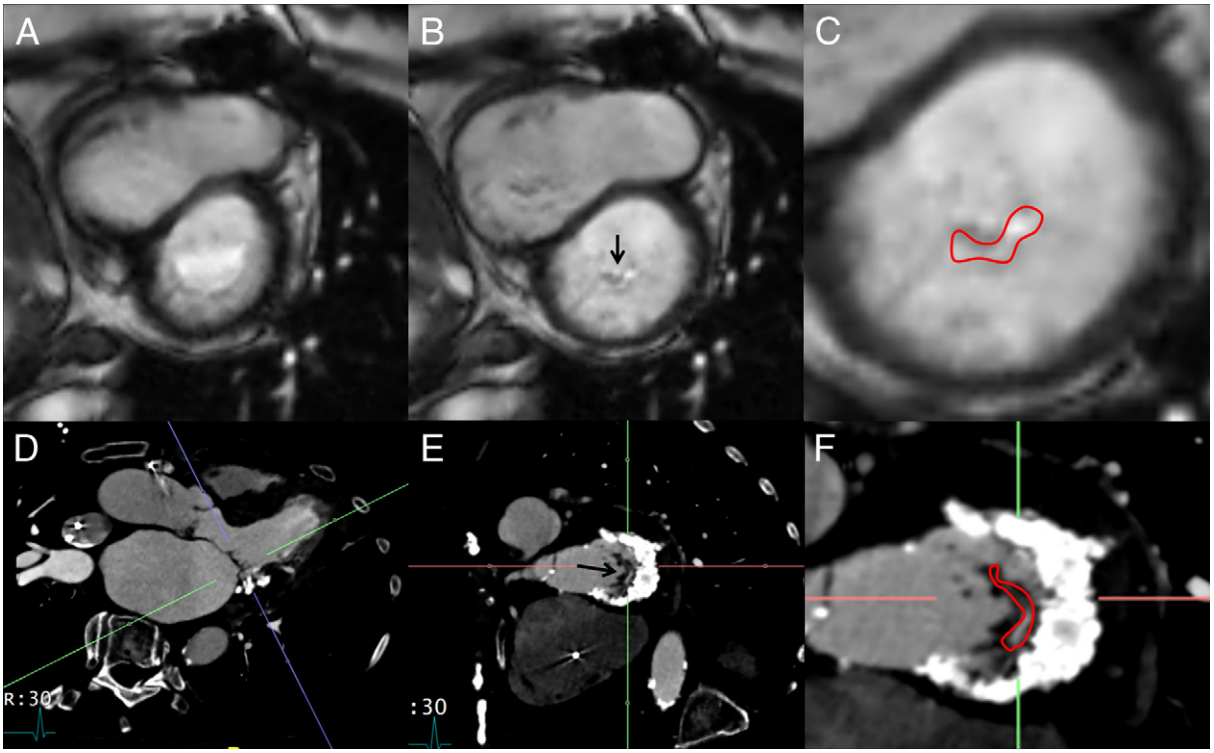

Figure 7 **Direct Planimetry of the Anatomic Regurgitant Orifice Using CMR and CCT**

(A to C) CMR SSFP short-axis cine **(A,** mid diastole; **B,** peak systole; and **C,** zoom of B with **red contour** denoting anatomic regurgitant orifice area [AROA]). **(D to F)** Cardiac computed tomography (multiplanar reformatting) with the use of long-axis view **(D)** to obtain an en face view of the AROA **(E)** for planimetry **(F)**.

Table 7 CMR and CCT Studies Using Direct Planimetry To Measure Anatomic Regurgitant Orifice Area

First Author, Year (Ref. #)	CMR or CT method	Reference Method(s)	N	Agreement	Accuracy	Reproducibility
Cardiac MRI studies						
Buchner et al., 2011 (57)	SSFP cine images at the valve plane	CMR RVol and RF by planimetry of LV and aortic PC imaging	74	With RF r = 0.80, RVol r = 0.80	—	—
Ozdogan et al., 2009 (22)	True FISP and FLASH short-axis cines	TTE EROA (by PISA)	21	With EROA True FISP r = 0.599, FLASH 0.715		—
Buchner et al., 2008 (34)	SSFP cine images at the valve plane	Catheterization (comparison with RVol and RF), echo PISA ERO, CMR RVol and RF*	35 (N-28 for RVol and RF comparison)	With catheterization MR severity grade r = 0.84, RF r = 0.86, RVol r = 0.83; with TTE PISA EROA r = 0.81; with CMR RF r = 0.91, RVol r = 0.90, MR severity r = 0.95	Compared to TTE EROA, CMR AROA higher by 16%, (range: −0.30 to 0.65 cm^2)	Inter 8 ± 7%†; intra 7 ± 6%†
Cardiac CT studies						
Arnous et al., 2011 (59)	64-Slice CT	TTE (length of regurgitant jet, VCW, PISA, RVol, and EROA)	23	Compared to TTE MR severity category r = 0.89, to echo EROA r = 0.50, with VC r = 0.48, no sig correlation with RVol by echo (from PISA)	Comparison with TTE EROA −0.02 ± 0.54 cm^2‡	—
Vural et al., 2010 (60)	16-Slice CT	TTE PISA EROA	26	Compared to EROA r = 0.89	Bias = 1.3 ± 14.5 mm^2‡ (p = NS)	—
Alkadhi et al., 2006 (58)	16-Slice CT	TEE (color jet area and extent, VCW§, CW density), and cardiac catheterization (visual criteria)	19	MR severity grading by TEE vs AROA Spearman r = 0.807, by ventriculography vs. AROA r = 0.922	—	—

*CMR RVol and RF by planimetry of LV and aortic phase contrast imaging. †Percentage variability (absolute value of the difference between 2 measurements divided by the mean of the 2 measurements). ‡Mean ± 2 SD. §Not consistent with ASE guidelines.
CCT = cardiac computed tomography; FISP = fast imaging with steady state precession; FLASH = fast low angle shot; MRI = magnetic resonance imaging; PC = phase contrast; SSFP = steady-state free precession; VCW = vena contract width; other abbreviations as in Tables 1 to 6.

all had small sample sizes and none reported reproducibility data.

Benefits and limitations of AROA by CMR and CCT. CCT can provide measurement of the AROA at the highest spatial resolution, while the spatial resolution of CMR is comparable to that with TTE. For the CMR acquisition, after recognition of the presence of MR, additional imaging, orthogonal to the jet direction (34), is required. The choice of this orthogonal plane can introduce interobserver variability in the measurement. Unless flow-sensitive cine GRE sequences or PC imaging is used, the presence of MR may be missed by the commonly used steady-state free precession cine sequences. Through-plane motion of the mitral annulus during systole makes it challenging to image the AROA. Finally, identification of the AROA can be difficult due to partial volume effects unless the orifice is very large.

With CCT, retrospective acquisition is necessary; this option is not attractive in the current era of prospectively triggered scanning with reduced radiation exposure. Even with retrospective acquisition, this measurement can be affected by limited temporal resolution. Although 2 of the 3 small studies (Table 7) show promising data, CCT should not be the primary method for AROA assessment. Finally, for both CMR and CCT, the cardiac phase in which the AROA should be measured for the various MR etiologies is unknown, as is the validity of these 2 techniques in patients with multiple MR jets.

Conclusions

The development of less invasive means of valve repair and replacement is likely to further augment the importance of MR quantitation in clinical practice. Although standard techniques for MR evaluation have been of value, their reproducibility and accuracy are limited in some patient groups. Although some of the new modalities may not be ready for adoption in all clinical imaging laboratories, this review documents their current validation. Recent technological advances in 3DE are likely to be the most suitable developments for widespread adoption, although CMR in appropriate settings may also play an important role. The role of CCT is still limited due to radiation exposure, lower temporal resolution, and the inability to assess flow. More work is needed to define the optimal strategy.

Reprint requests and correspondence: Dr. Thomas H. Marwick, Cleveland Clinic Foundation, Cardiovascular Imaging J1-5, Heart and Vascular Institute, 9500 Euclid Avenue, Cleveland, Ohio 44195. E-mail: marwict@ccf.org.

REFERENCES

1. Nkomo VT, Gardin JM, Skelton TN, Gottdiener JS, Scott CG, Enriquez-Sarano M. Burden of valvular heart diseases: a population-based study. Lancet 2006;368:1005–11.
2. Avierinos JF, Gersh BJ, Melton LJ III, et al. Natural history of asymptomatic mitral valve prolapse in the community. Circulation 2002;106:1355–61.

3. Enriquez-Sarano M, Avierinos JF, Messika-Zeitoun D, et al. Quantitative determinants of the outcome of asymptomatic mitral regurgitation. N Engl J Med 2005;352:875–83.
4. Tribouilloy CM, Enriquez-Sarano M, Schaff HV, et al. Impact of preoperative symptoms on survival after surgical correction of organic mitral regurgitation: rationale for optimizing surgical indications. Circulation 1999;99:400–5.
5. Bonow RO, Carabello BA, Chatterjee K, et al. ACC/AHA 2006 guidelines for the management of patients with valvular heart disease: a report of the American College of Cardiology/American Heart Association Task Force on Practice Guidelines (writing Committee to Revise the 1998 guidelines for the management of patients with valvular heart disease) developed in collaboration with the Society of Cardiovascular Anesthesiologists endorsed by the Society for Cardiovascular Angiography and Interventions and the Society of Thoracic Surgeons. J Am Coll Cardiol 2006;48:e1–148.
6. Tribouilloy C, Shen WF, Quere JP, et al. Assessment of severity of mitral regurgitation by measuring regurgitant jet width at its origin with transesophageal Doppler color flow imaging. Circulation 1992; 85:1248–53.
7. Kahlert P, Plicht B, Schenk IM, Janosi RA, Erbel R, Buck T. Direct assessment of size and shape of noncircular vena contracta area in functional versus organic mitral regurgitation using real-time three-dimensional echocardiography. J Am Soc Echocardiogr 2008;21:912–21.
8. Marsan NA, Westenberg JJ, Ypenburg C, et al. Quantification of functional mitral regurgitation by real-time 3D-echocardiography: comparison with 3D-velocity-encoded cardiac magnetic resonance. JACC Cardiovasc Imaging 2009;2:1245–52.
9. Mele D, Vandervoort P, Palacios I, et al. Proximal jet size by Doppler color flow mapping predicts severity of mitral regurgitation. Clinical studies. Circulation 1995;91:746–54.
10. Zeng X, Levine RA, Hua L, et al. Diagnostic value of vena contracta area in the quantification of mitral regurgitation severity by color Doppler 3D-echocardiography. Circ Cardiovasc Imaging 2011;4:506–13.
11. Iwakura K, Ito H, Kawano S, et al. Comparison of orifice area by transthoracic three-dimensional Doppler echocardiography versus proximal isovelocity surface area (PISA) method for assessment of mitral regurgitation. Am J Cardiol 2006;97:1630–7.
12. Shanks M, Siebelink HM, Delgado V, et al. Quantitative assessment of mitral regurgitation: comparison between three-dimensional transesophageal echocardiography and magnetic resonance imaging. Circ Cardiovasc Imaging 2010;3:694–700.
13. Yosefy C, Hung J, Chua S, et al. Direct measurement of vena contracta area by real-time 3-dimensional echocardiography for assessing severity of mitral regurgitation. Am J Cardiol 2009;104:978–83.
14. Little SH, Pirat B, Kumar R, et al. Three-dimensional color Doppler echocardiography for direct measurement of vena contracta area in mitral regurgitation: in vitro validation and clinical experience. J Am Coll Cardiol Img 2008;1:695–704.
15. Khanna D, Vengala S, Miller AP, et al. Quantification of mitral regurgitation by live three-dimensional transthoracic echocardiographic measurements of vena contracta area. Echocardiography 2004; 21:737–43.
16. Marsan NA, Westenberg JJ, Roes SD, et al. Three-dimensional echocardiography for the preoperative assessment of patients with left ventricular aneurysm. Ann Thorac Surg 2011;91:113–21.
17. Buck T, Plicht B, Kahlert P, Schenk IM, Hunold P, Erbel R. Effect of dynamic flow rate and orifice area on mitral regurgitant stroke volume quantification using the proximal isovelocity surface area method. J Am Coll Cardiol 2008;52:767–78.
18. Hung J, Otsuji Y, Handschumacher MD, Schwammenthal E, Levine RA. Mechanism of dynamic regurgitant orifice area variation in functional mitral regurgitation: physiologic insights from the proximal flow convergence technique. J Am Coll Cardiol 1999;33:538–45.
19. Yoganathan AP, Cape EG, Sung HW, Williams FP, Jimoh A. Review of hydrodynamic principles for the cardiologist: applications to the study of blood flow and jets by imaging techniques. J Am Coll Cardiol 1988;12:1344–53.
20. Krombach GA, Kuhl H, Bucker A, et al. Cine MR imaging of heart valve dysfunction with segmented true fast imaging with steady state free precession. J Magn Reson Imaging 2004;19:59–67.
21. Pflugfelder PW, Sechtem UP, White RD, Cassidy MM, Schiller NB, Higgins CB. Noninvasive evaluation of mitral regurgitation by analysis of left atrial signal loss in cine magnetic resonance. Am Heart J 1989;117:1113–9.
22. Ozdogan O, Yuksel A, Gurgun C, Kayikcioglu M, Yavuzgil O, Cinar CS. Evaluation of the severity of mitral regurgitation by the use of signal void in magnetic resonance imaging. Echocardiography 2009; 26:1127–35.
23. Wagner S, Auffermann W, Buser P, et al. Diagnostic accuracy and estimation of the severity of valvular regurgitation from the signal void on cine magnetic resonance images. Am Heart J 1989;118:760–7.
24. Sechtem U, Pflugfelder PW, Cassidy MM, et al. Mitral or aortic regurgitation: quantification of regurgitant volumes with cine MR imaging. Radiology 1988;167:425–30.
25. Thavendiranathan P, Liu S, Datta S, et al. Automated quantification of mitral inflow and aortic outflow stroke volumes by three-dimensional real-time volume color-flow Doppler transthoracic echocardiography: comparison with pulsed-wave Doppler and cardiac magnetic resonance imaging. J Am Soc Echocardiogr 2012;25:56–65.
26. Lodato JA, Weinert L, Baumann R, et al. Use of 3-dimensional color Doppler echocardiography to measure stroke volume in human beings: comparison with thermodilution. J Am Soc Echocardiogr 2007;20: 103–12.
27. Ge S, Bu L, Zhang H, et al. A real-time 3-dimensional digital Doppler method for measurement of flow rate and volume through mitral valve in children: a validation study compared with magnetic resonance imaging. J Am Soc Echocardiogr 2005;18:1–7.
28. Lu X, Nadvoretskiy V, Klas B, et al. Measurement of volumetric flow by real-time 3-dimensional doppler echocardiography in children. J Am Soc Echocardiogr 2007;20:915–20.
29. Matthews F, Largiader T, Rhomberg P, van der Loo B, Schmid ER, Jenni R. A novel operator-independent algorithm for cardiac output measurements based on three-dimensional transoesophageal colour Doppler echocardiography. Eur J Echocardiogr 2010;11:432–7.
30. Pemberton J, Jerosch-Herold M, Li X, et al. Accuracy of real-time, three-dimensional Doppler echocardiography for stroke volume estimation compared with phase-encoded MRI: an in vivo study. Heart 2008;94:1212–3.
31. Pemberton J, Li X, Kenny A, Davies CH, Minette MS, Sahn DJ. Real-time 3-dimensional Doppler echocardiography for the assessment of stroke volume: an in vivo human study compared with standard 2-dimensional echocardiography. J Am Soc Echocardiogr 2005;18:1030–6.
32. Thavendiranathan P, Liu S, Datta S, et al. Automated 3d-quantification of mitral regurgitation by real-time volume color flow doppler: comparison with cardiac magnetic resonance imaging. J Am Soc Echocardiogr 2011;24:B3.
33. Myerson SG, Francis JM, Neubauer S. Direct and indirect quantification of mitral regurgitation with cardiovascular magnetic resonance, and the effect of heart rate variability. MAGMA 2010;23:243–9.
34. Buchner S, Debl K, Poschenrieder F, et al. Cardiovascular magnetic resonance for direct assessment of anatomic regurgitant orifice in mitral regurgitation. Circ Cardiovasc Imaging 2008;1:148–55.
35. Hundley WG, Li HF, Willard JE, et al. Magnetic resonance imaging assessment of the severity of mitral regurgitation. Comparison with invasive techniques. Circulation 1995;92:1151–8.
36. Kizilbash AM, Hundley WG, Willett DL, Franco F, Peshock RM, Grayburn PA. Comparison of quantitative Doppler with magnetic resonance imaging for assessment of the severity of mitral regurgitation. Am J Cardiol 1998;81:792–5.
37. Guo YK, Yang ZG, Ning G, et al. Isolated mitral regurgitation: quantitative assessment with 64-section multidetector CT—comparison with MR imaging and echocardiography. Radiology 2009;252:369–76.
38. Kon MW, Myerson SG, Moat NE, Pennell DJ. Quantification of regurgitant fraction in mitral regurgitation by cardiovascular magnetic resonance: comparison of techniques. J Heart Valve Dis 2004;13: 600–7.
39. Glogar D, Globits S, Neuhold A, Mayr H. Assessment of mitral regurgitation by magnetic resonance imaging. Magn Reson Imaging 1989;7:611–7.
40. Fujita N, Chazouilleres AF, Hartiala JJ, et al. Quantification of mitral regurgitation by velocity-encoded cine nuclear magnetic resonance imaging. J Am Coll Cardiol 1994;23:951–8.
41. Gelfand EV, Hughes S, Hauser TH, et al. Severity of mitral and aortic regurgitation as assessed by cardiovascular magnetic resonance: opti-

mizing correlation with Doppler echocardiography. J Cardiovasc Magn Reson 2006;8:503–7.
42. Gatehouse PD, Rolf MP, Graves MJ, et al. Flow measurement by cardiovascular magnetic resonance: a multi-centre multi-vendor study of background phase offset errors that can compromise the accuracy of derived regurgitant or shunt flow measurements. J Cardiovasc Magn Reson 2010;12:5.
43. Kilner PJ, Gatehouse PD, Firmin DN. Flow measurement by magnetic resonance: a unique asset worth optimising. J Cardiovasc Magn Reson 2007;9:723–8.
44. Yosefy C, Levine RA, Solis J, Vaturi M, Handschumacher MD, Hung J. Proximal flow convergence region as assessed by real-time 3-dimensional echocardiography: challenging the hemispheric assumption. J Am Soc Echocardiogr 2007;20:389–96.
45. Plicht B, Kahlert P, Goldwasser R, et al. Direct quantification of mitral regurgitant flow volume by real-time three-dimensional echocardiography using dealiasing of color Doppler flow at the vena contracta. J Am Soc Echocardiogr 2008;21:1337–46.
46. Breburda CS, Griffin BP, Pu M, Rodriguez L, Cosgrove DM III, Thomas JD. Three-dimensional echocardiographic planimetry of maximal regurgitant orifice area in myxomatous mitral regurgitation: intraoperative comparison with proximal flow convergence. J Am Coll Cardiol 1998;32:432–7.
47. Lange A, Palka P, Donnelly J, Burstow D. Quantification of mitral regurgitation orifice area by 3-dimensional echocardiography: comparison with effective regurgitant orifice area by PISA method and proximal regurgitant jet diameter. Int J Cardiol 2002;86:87–98.
48. Chandra S, Salgo IS, Sugeng L, et al. A three-dimensional insight into the complexity of flow convergence in mitral regurgitation: adjunctive benefit of anatomic regurgitant orifice area. Am J Physiol Heart Circ Physiol 2011;301:H1015–24.
49. Sitges M, Jones M, Shiota T, et al. Real-time three-dimensional color doppler evaluation of the flow convergence zone for quantification of mitral regurgitation: Validation experimental animal study and initial clinical experience. J Am Soc Echocardiogr 2003;16:38–45.
50. Matsumura Y, Fukuda S, Tran H, et al. Geometry of the proximal isovelocity surface area in mitral regurgitation by 3-dimensional color Doppler echocardiography: difference between functional mitral regurgitation and prolapse regurgitation. Am Heart J 2008;155:231–8.
51. Little SH, Igo SR, Pirat B, et al. In vitro validation of real-time three-dimensional color Doppler echocardiography for direct measurement of proximal isovelocity surface area in mitral regurgitation. Am J Cardiol 2007;99:1440–7.
52. Matsumura Y, Saracino G, Sugioka K, et al. Determination of regurgitant orifice area with the use of a new three-dimensional flow convergence geometric assumption in functional mitral regurgitation. J Am Soc Echocardiogr 2008;21:1251–6.
53. Grady L, Datta S, Kutter O, et al. Regurgitation quantification using 3D-PISA in volume echocardiography. Med Image Comput Comput Assist Interv 2011;14:512–9.
54. Francis DP, Willson K, Ceri Davies L, Florea VG, Coats AJ, Gibson DG. True shape and area of proximal isovelocity surface area (PISA) when flow convergence is hemispherical in valvular regurgitation. Int J Cardiol 2000;73:237–42.
55. Schwammenthal E, Chen C, Benning F, Block M, Breithardt G, Levine RA. Dynamics of mitral regurgitant flow and orifice area. Physiologic application of the proximal flow convergence method: clinical data and experimental testing. Circulation 1994;90:307–22.
56. Altiok E, Hamada S, van Hall S, et al. Comparison of direct planimetry of mitral valve regurgitation orifice area by three-dimensional transesophageal echocardiography to effective regurgitant orifice area obtained by proximal flow convergence method and vena contracta area determined by color Doppler echocardiography. Am J Cardiol 2011;107:452–8.
57. Buchner S, Poschenrieder F, Hamer OW, et al. Direct visualization of regurgitant orifice by CMR reveals differential asymmetry according to etiology of mitral regurgitation. JACC Cardiovasc Imaging 2011;4:1088–96.
58. Alkadhi H, Wildermuth S, Bettex DA, et al. Mitral regurgitation: quantification with 16-detector row CT—initial experience. Radiology 2006;238:454–63.
59. Arnous S, Killeen RP, Martos R, Quinn M, McDonald K, Dodd JD. Quantification of mitral regurgitation on cardiac computed tomography: comparison with qualitative and quantitative echocardiographic parameters. J Comput Assist Tomogr 2011;35:625–30.
60. Vural M, Ucar O, Celebi OO, et al. Evaluation of effective regurgitant orifice area of mitral valvular regurgitation by multislice cardiac computed tomography. J Cardiol 2010;56:236–9.

Key Words: 3D-echocardiography ■ cardiac magnetic resonance imaging ■ cardiac computed tomography ■ mitral regurgitation ■ quantification.